Published in final edited form as:
J Immunol. 2013 February 15; 190(4): 1433–1446. doi:10.4049/jimmunol.1200824.

Prolonged apoptotic cell accumulation in germinal centers of Mer-deficient mice causes elevated B cell and CD4+ helper T cell responses leading to autoantibody production

Tahsin N. Khan[*,†], **Eric B. Wong**[*,†], **Chetna Soni**[*,†], and **Ziaur S.M. Rahman**[*,†,2]

[*]Department of Microbiology and Immunology, Thomas Jefferson University, Jefferson Medical College, Philadelphia, PA

[†]Department of Microbiology and Immunology, Pennsylvania State University College of Medicine, Hershey, PA

Abstract

Mer (MerTK) is a member of the Tyro-3/Axl/Mer (TAM) subfamily of receptor tyrosine kinases and its expression on phagocytes facilitates their clearance of apoptotic cells (ACs). Mer expression in germinal centers (GCs) occurs predominantly on tingible body macrophages (TBMϕs). B and T cells do not express Mer. Here, we show that Mer deficiency (Mer−/−) resulted in the long-term accumulation of ACs primarily in GCs and not in the T cell zone, marginal zone or red pulp areas of the spleen. AC accumulation in GCs led to augmented AFC, GC and IgG2 Ab responses in Mer−/− mice, which were sustained for at least 80 days. Enhanced responses in Mer −/− mice were due to increased activation and proliferation of B cells and $CD4^+$ helper T cells including follicular helper T (T_{FH}) cells, which resulted in high titers of anti-nuclear antibodies (ANAs) in Mer−/− mice compared to wild type (WT) controls. Secondary IgG-producing AFC, total IgG and IgG2 Ab responses were also increased in Mer−/− mice. Finally, compared to WT controls, Mer−/− mice had increased percentage of IFN-γ producing $CD4^+$ helper T cells and elevated levels of Th1 (i.e., IL-2 and IFN-γ) and pro-inflammatory (i.e., TNF and IL-6) cytokines, consistent with elevated levels of Th1-biased IgG2 Abs in Mer−/− mice. Together, our results demonstrate that Mer deficiency induces prolonged accumulation of ACs in GCs resulting in dysregulation of GC B cell and $CD4^+$ helper T cell responses and Th1 cytokine production leading to alteration of B cell tolerance and the development of autoantibodies.

Keywords

Mer; MerTK; germinal center; B cells; apoptotic cells

Introduction

Efficient clearance of apoptotic cells (ACs) generated systemically in numerous ways appears to be an essential step for the immune system to maintain tissue homeostasis (1). Clearance of ACs generated in germinal centers (GCs) as a result of negative selection of low affinity and autoreactive B cells may also be necessary to regulate B and/or T cell responses against foreign-Ag, as well as to maintain immune tolerance to self-Ag. Inefficient clearance of ACs results in the development of autoantibodies and autoimmunity (2–5). We recently showed that tingible body macrophages (TBMϕs) in GCs are the primary

[2]Address correspondence and reprint requests to: Dr. Ziaur Rahman, Department of Microbiology and Immunology, H107, Pennsylvania State University College of Medicine, 500 University Drive, Hershey, PA 17033-0850. zrahman@hmc.psu.edu.

phagocytes which express Mer and are associated with the clearance of ACs generated within GCs (6).

Several studies in mice have suggested the role of TBMϕs in regulating the GC response and in maintaining peripheral B cell tolerance (2, 6–8). The presence of ACs during monocyte activation increases their secretion of the anti-inflammatory cytokine IL-10 and decreases secretion of the pro-inflammatory cytokines TNF-α, IL-1 and IL-12 (9, 10). Likewise, the phagocytosis of ACs by TBMϕs in GCs may potentially mediate the induction of anti-inflammatory cytokines IL-10 and TGF-β, which, in turn, may help negatively regulate B cells including autoreactive cells that are present in GCs. On the other hand, in the absence of efficient clearance, ACs in GCs may progress to the late stage of apoptotic cell death (termed secondary necrosis) and pose a threat to immune regulation and tolerance by promoting the production of pro-inflammatory cytokines. While TBMϕs regulate GC response and tolerance by clearing ACs generated in GCs, the phagocytosis of injected ACs by marginal zone macrophages (MZMs) were previously shown to maintain MZ B cell tolerance as depletion of MZMs led to pro-inflammatory cytokine production and accelerated autoimmune disease progression in lupus-prone mice (11, 12).

A number of receptors that mediate phagocytosis and clear ACs include TAM (TAM: Tyro-3, Axl, and Mer/MerTK) subfamily of tyrosine kinase receptors, $\alpha_v\beta_3$-integrin, T cell immunoglobulin-4 (Tim-4) and CD36 (1, 13–15). Several soluble dual-function bridging proteins including milk fat globule EGF factor 8 (MFG-E8), growth arrest specific 6 (Gas-6), protein S and complement factor C1q have been implicated in facilitating AC phagocytosis. These dual-function bridging molecules are capable of binding both ligands (i.e., phosphatidylserine) exposed on the surface of ACs and their corresponding receptors expressed on phagocytes. TAM receptors primarily utilize Gas-6 and protein S (16–18). While Tim-4 directly binds phosphatidylserine expressed on ACs (15), the $\alpha_v\beta_3$-integrin pathway uses MFG-E8 for engulfing ACs (19).

Mer tyrosine kinase receptor (MerTK or Mer) expression on phagocytes (i.e., Mϕs and DCs) facilitates macrophage and DC clearance of ACs (16, 18, 20, 21). Mer appears to be necessary for the maintenance of self-tolerance, as a lupus-like syndrome occurs in mice lacking the Mer receptor (Mer−/−) (3). The development of autoimmunity in these mice is believed to be due to the delayed clearance of ACs and dysregulated cytokine production by macrophages and DCs (22). Recent studies by the Cohen group have indicated an enhanced marginal zone (MZ) B cell response to type II T-independent Ag in Mer−/− mice (21). Loss of tolerance of DNA-specific Ig heavy chain transgenic 3H9 B cells that primarily develop into MZ B cell phenotype has also been described in Mer−/− mice (23). Recently, in an analysis of the early immune response (9, 14 and 21 days post-immunization) against the T cell dependent-Ag (TD-Ag) NP-CGG we showed enhanced AFC, GC and IgG2 Ab responses in Mer−/− mice compared to control animals (6). We also observed an accumulation of ACs in GCs at this time point due to lack of Mer expression on TBMϕs (6). While impaired clearance of ACs in GCs appeared to drive elevated AFC, GC and IgG2 Ab responses at earlier time points (6), the role for the GC as a site of long-term accumulation of uncleared apoptotic debris which may lead to a break in peripheral B cell tolerance and production of anti-nuclear antibodies (ANA) in Mer−/− mice is not clear.

In this study, we determined whether AC accumulation in GCs and elevated AFC, GC and IgG2 Ab responses caused by Mer deficiency sustained for an extended period of time, which consequently harbored the generation of autoreactive B cells and production of high titers of ANA. We also evaluated whether enhanced responses and AC accumulation in GCs of Mer−/− mice were a result of increased B and helper T cell responses, especially GC B cells and T_{FH} cells. We observed high titers of ANAs in Mer−/− mice compared to WT

controls, indicating a break in B cell tolerance in the presence of AC accumulation in Mer−/− GCs. We found significantly increased activation and proliferation of GC B cells and $CD4^+$ effector helper T cell responses including T_{FH} cells that were associated with AC accumulation in Mer−/− GCs compared to WT controls. Mer deficiency also resulted in a significant increase in the generation of long-lived primary (IgG^+ AFC, GC, T_{FH} cell, IgG and IgG2 Ab) and memory (IgG^+ AFC, IgG and IgG2 Ab) responses compared to WT controls. Finally, we observed a significant increase in IFN-γ production by $CD4^+$ helper T cells obtained from NP-OVA immunized Mer−/− mice compared to WT controls. These data reinforce a crucial role of Mer-mediated clearance of ACs from GCs in regulating peripheral B cell, $CD4^+$ helper T cell and autoantibody responses and therefore, having major implications in loss of peripheral B cell tolerance and the induction of autoimmunity.

Materials and Methods

Mice

Mice deficient in Mer/MerTK receptor tyrosine kinase on a F2 hybrid background of C57BL/6 (B6) and 129 mice (B6.129Mertk^{tm1Grl}/J) (designated Mer−/−) and wild type (WT) controls with identical background (B6.129F2/J) were purchased from the Jackson Laboratory (Bar Harbor, ME). Subsequently, F3 mice of both Mer−/− and WT controls were generated by crossing F2 males and females of each genotype and maintained in a pathogen-free facility. All experimental procedures performed on these animals were conducted according to the guidelines of our Institutional Animal Care and Use Committee. All mice were 7–9 weeks old at the time of immunization.

Immunization procedure

T-dependent Ag (4-hydroxy-3-nitrophenyl) acetyl $(NP)_{16}$-ovalbumin (OVA) NP_{16} OVA (Biosearch Technologies, Novato, CA) was precipitated with 10% alum. Mer−/− and WT control mice were immunized (i.p.) twice with NP_{16}-OVA/alum: on day 0 (with 100 μg per mouse) and then again on day 7 (with 50 μg). At multiple time points post-immunization, mouse spleens and/or bone marrow were harvested for various analyses. For measuring Ab titers, serum samples were collected from these mice on days 0, 14, 21, 28, 45, 60 and 80 post-immunization. To study secondary responses, mice were rested for 80 days post-immunization and analyzed four days after boosting with 50 μg NP-OVA in PBS.

Reagents and antibodies for flow cytometry

Pacific blue-anti-B220 (RA3-6B2); PeCy7-anti-CD95 (Fas) (Jo2); Alexa Fluor 700-anti-CD4 (RM4-5); PE-anti-PD-1 (J43); biotin-anti-CXCR5 (2G8) (BD Pharmingen, San Diego, CA); PerCP-Cy5.5-anti-CD69 (H1.253); PE-Cy5-anti-CD86 (GL1); APC-anti-CD44 (IM7); PE-Cy7-anti-CD62L (MEL-14); PE-Cy5-streptavidin (SA); PE-anti-CD80 (16–10A1); APC-Cy7- anti-CD25 (PC61); FITC-anti-INF-γ (XMG1.2); APC-anti-IL-4(11B11) (eBioscience, San Diego, CA); FITC-peanut-agglutinin (PNA) (Sigma-Aldrich, St. Louis, MO).

Reagents and antibodies for immunohistology

FITC-GL7; Biotin-rat anti-mouse IgD (11–26c, Southern Biotech, Birmingham, AL); Biotin-anti-BrdU (Bu20a); Purified anti-mouse Tim-4 (RMT4-54) (Biolegend, San Diego, CA); HRP-peanut-agglutinin (PNA) (Sigma-Aldrich, St. Louis, MO); Biotin-mouse anti-rat IgG; Alexa Fluor 488 anti-Armenian hamster IgG (Jackson Immunoresearch Laboratories, West Grove, PA); Alkaline phosphatase (AP)-streptavidin (SA); AP Blue substrate kit III; Vector NovaRED substrate kit (Vector Laboratories, Burlingame, CA); RPE-(red phycoerythrin) and Alexa Flour 647-anti-CD68 (AbD Serotec, Raleigh, NC); Affinity-

purified anti-mouse Tyro-3 and Axl (R&D Systems, Minneapolis, MN); Biotin-rat anti-mouse MOMA-1 (Abcam, Cambridge, MA); Purified rat anti-mouse Ki67 (ImmunoKontact, Abingdon, UK).

Flow cytometry

Multi-color flow cytometric analysis was performed on single cell suspensions prepared from spleens of immunized mice stained with different combinations of the Abs listed above. Biotinylated Abs were detected with streptavidin-conjugated fluorochromes. Stained cells were analyzed using the BD LSRII analyzer. Data were analyzed using FlowJo software (Treestar, San Carlos, CA).

Immunohistology and Terminal Deoxynucleotidyl Transferase dUTP Nick End Labeling (TUNEL) assay

Preparation of spleen cryostat sections (5–6 microns) and immunohistological analysis were performed using the Abs and reagents as previously described (24). TUNEL (Terminal deoxynucleotidyl Transferase dUTP Nick End Labeling) Kit and Apoptag Peroxidase In Situ Apoptosis detection Kit (Millipore, Temecula, CA) were used to perform apoptosis detection assays on the spleen sections following the manufacturer's instructions. The stained spleen sections using both the kits were analyzed using a fluorescence microscope (Leica Microsystems, Buffalo Grove, IL) and images were captured as described (6). The color intensity of the images was slightly enhanced by Adobe Photoshop (Adobe Systems Inc. San Jose, CA), which was necessary for improved visualization and was carried out consistently between Mer−/− and WT controls, while maintaining the integrity of the data. The magnification of the images was 50x, 100x or 200x as indicated in the figure legends.

In vivo B cell proliferation assay

B cell proliferation in GCs was examined using two different methods: (a) *In situ* BrdU proliferation assay and (b) *In situ* intracellular staining of B cells for Ki67. The *in situ* BrdU proliferation assay was performed using a kit (BD Biosciences, Franklin Lakes, NJ). Mice were immunized with NP-OVA as described above. On day 21 (d21) post-first immunization, BrdU (1 mg/mouse) was administered i.p. 1–2hr prior to the sacrificing and freezing spleens. One of two consecutive spleen sections (5–6 μm) was stained with anti-IgD and PNA. Alkaline-phosphatase (AP)-conjugated IgD and horseradish peroxidase (HRP)-labeled PNA were developed using the Blue Alkaline Phosphatase Substrate Kit III and NovaRed Substrate Kit (both from Vector Laboratories, Burlingame, CA), respectively. BrdU uptake was detected on the other section following manufacturer's instruction. Bromodeoxyuridinepositive ($BrdU^+$) cells in GCs were counted by two individuals with randomly picked GCs from several WT and Mer−/− mice. A two-color immunofluorescent staining with anti-Ki67 (a proliferation marker) and GC B cell marker GL7 was performed on spleen sections obtained on d21 post-NP-OVA immunization as described above.

ELISpot assays

ELISpot assays were performed as described (6). Briefly, splenocytes and/or bone marrow single cell suspensions from NP-OVA immunized Mer−/− mice and WT controls were plated at 1×10^6 cells/well and diluted serially (1:2) in NP_{11}-BSA coated multiscreen 96-well filtration plates (Millipore, Bedford, MA) for 6hr at 37°C and 4% CO_2. NP-specific IgM Abs produced by AFCs were detected using biotinylated anti-mouse IgM (Jackson Immunoresearch, West Grove, PA) and streptavidin (SA)-alkaline phosphatase (AP, Vector Laboratories, Burlingame, CA). NP-specific IgG Abs produced by AFCs were detected using alkaline-phosphatase-conjugated IgG (Molecular Probes, Eugene, OR). Plates were developed using the Vector Blue Alkaline-Phosphatase Substrate Kit III (Vector

Laboratories, Burlingame, CA). ELISpots were counted using a computerized imaging video system (Cellular Technology, Cleveland, OH).

ELISA

NP-specific serum Abs were measured in sera from immunized mice as described (25). To measure NP-specific total serum Ab titers of different isotypes and subtypes [such as IgM (Jackson Immunoresearch, West Grove, PA), IgG (Biolegend, San Diego, CA), IgG1 (Molecular Probes, Eugene, OR) and IgG2 (Sigma-Aldrich, St. Louis, MO)] ELISA plates were coated with NP_{11}-BSA (10 μg/ml). To measure ANA titers, plates were coated with dsDNA (20 μg/ml), histone (10 μg/ml) or nucleosome (mixture of dsDNA and histone). Biotinylated antibodies were detected by streptavidin (SA)-alkaline phosphatase (Vector Laboratories, Burlingame, CA). The plates were developed by the PNPP (*p*-Nitrophenyl Phosphate, Disodium Salt) (Thermo Fisher Scientific, Rockford, IL) substrates for alkaline phosphatase. Serum samples were first diluted in PBS and then subsequently threefold serial dilution was carried out for each sample. The dilution factor for each sample was generated in a logarithmic scale via the software named “Origin” (OriginLab Corp, Northampton, MA) as described (6).

Ex vivo B and T cell proliferation assay

Naive B and T cells were purified from splenocytes of WT and Mer−/−mice 10 days after immunization with NP-OVA, by negative selection using mouse Pan T cell Isolation Kit II and anti-CD43 (Ly-48) microbeads respectively, using magnetic cell separation (Miltenyi Biotec, Germany). Purified cells were intracellularly stained with 3 μM CellTrace Violet (Invitrogen, Carlsbad, CA) as per manufacturer’s instructions. Stained T cells were then cultured with 10 μg/ml plate bound anti-CD3 and 2 μg/ml soluble anti-CD28 antibody (BioLegend, San Diego, CA) in RPMI supplemented with 10% FBS while stained B cells were cultured with 25 μg/ml soluble anti-IgM (Jackson ImmunoResearch, Baltimore Pike, PA) and 5 μg/ml soluble anti-CD40 antibody (BioLegend) in a round bottom 96 well plate for different time periods. CellTrace-stained or unstained, unstimulated purified B and T cells were used as control in the assay. After 72hr or 96hr of stimulation, cells were harvested, washed and fixed with 2% paraformaldehyde and subjected to flow cytometric analysis with the BD LSRII analyzer. Data were acquired using FACSDiva software (BD Biosciences, San Jose, CA) and analyzed by FlowJo software (Tree Star, San Carlos, CA). Proliferating cells were scored by quantifying the reduction in CellTrace Violet fluorescence intensity in dividing cells as compared to stained unactivated control cells.

Ex vivo T cell stimulation and intracellular staining for cytokines

7–9 wk old WT and Mer−/− mice were immunized with NP-OVA as described above. Splenocytes were harvested on days 10 and 15 post-immunization. Cells were plated at 0.5×10^6 cells/well in 96-well plate and stimulated with PMA (10 ng/ml) and Ionomycin (0.5 μg/ml). GolgiStop (BD Biosciences, San Jose, CA) was added according to manufacturer’s guidelines. Cells were harvested at 0, 4 and 8 hr post-stimulation and stained intracellularly to measure cytokine production. Stained cells were analyzed using a BD LSR II (BD Biosciences, San Jose, CA) analyzer. Data were analyzed using FlowJo software (Tree Star, San Carlos, CA).

Determination of Th1, Th2 and pro-inflammatory cytokine levels

Purified T cells (2.5×10^6/ml) obtained from NP-OVA immunized WT and Mer−/− mice 10 days after immunization were activated with PMA (10 ng/ml) and Ionomycin (0.5 ug/ml) in RPMI supplemented with 10% FBS in 96 well plates. The supernatant from the activated cells was harvested at 24hr and 48hr post-stimulation and used for the quantification of

secreted cytokines. Levels of Th1/Th2/Th17 cytokines were determined by flow cytometry using the BD™ Cytometric Bead Array (CBA) mouse Th1/Th2/Th17 cytokine kit (BD Biosciences, Franklin Lake, NJ), following manufacturer's instructions. The cytokine concentrations were quantified by standard curves plotted using a five-parameter logistic curve-fitting model, using BD FCAPArray software (San Jose, California). Samples with cytokine concentration below the detection limit for the assay have been arbitrarily assigned a value of 1 pg/ml.

Statistical analysis

Statistical analysis was performed using Student's *t*-test. P values of <0.05, <0.01, and <0.001 are depicted as *, **, and *** respectively. *P* values less than 0.05 (<0.05) were considered significant.

Results

Long-term accumulation of ACs occurs predominantly in GCs and not in the T cell zone, marginal zone or red pulp area of the spleen in Mer−/− mice

By evaluating an earlier time point (day14) of the GC response against TD-Ag we have recently shown that ACs accumulate in GCs of Mer−/− mice in the absence of Mer-mediated clearance of dead and/or dying cells by TBMϕs (6). However, it is not clear whether ACs continue to accumulate in GCs of Mer−/− mice over time, which in turn, may alter peripheral B cell tolerance at the GC checkpoint that leads to autoantibody production in Mer−/− mice. To study potential accumulation of ACs in Mer−/− GCs over an extended period of time, we immunized Mer−/− mice and their WT counterparts with the TD-Ag NP-OVA. We used a modified version of the repeated immunization protocol (described in Materials and Methods) previously shown to induce a robust GC response (2). According to this protocol, mice were immunized (i.p.) with 100 μg at day 0 and again one week later with 50 μg NP-OVA in alum. Spleens from Mer−/− and WT control mice were harvested at 21 and 80 days after first immunization.

Spleen sections of NP-OVA-immunized WT mice stained with GL7 (green, GC B cell marker), anti-CD68 (red, a marker for TBMϕs) and TUNEL (blue, apoptotic cell detection assay) exhibited very few $TUNEL^+$ ACs in GCs (defined by dashed lines) 21 and 80 days after immunization (2^{nd} and 3^{rd} panels in 1^{st} and 3^{rd} rows, Fig. 1A and B). In contrast, we found a marked increase in $TUNEL^+$ ACs in GCs of Mer−/− mice up to day 80 (2^{nd} and 3^{rd} panels in 2^{nd} and 4^{th} rows, Fig. 1A and B). The $TUNEL^+$ ACs continued to be predominantly localized outside of $CD68^+$ TBMϕs within Mer−/− GCs at least up to day 80.

The B cell follicle, T cell zone, marginal zone and red pulp are four distinct sites in the spleen where potential AC accumulation in the absence of Mer may influence B cells, T cells and APCs. Therefore, to study the overall distribution of AC accumulation in NP-OVA immunized Mer−/− spleen, we performed immunohistology on two consecutive spleen sections obtained on day 21 post-immunization of WT and Mer−/−mice. One was stained with anti-IgD and TUNEL (1^{st} and 3^{rd} panels, Fig. 1C) and the other was stained with MOMA-1 and TUNEL (2^{nd} and 4^{th} panels, Fig. 1C). GCs (highlighted by the dashed yellow lines) are defined as IgD^{neg}. MOMA-1 stains for metallophillic macrophages which defines the border between B cell follicles and marginal zone. Low magnification (100x) representative images in this analysis revealed very few $TUNEL^+$ cells outside of GCs (i.e., red pulp, MZ or T cell zones) in Mer−/−spleen (Fig. 1C, right) indicating predominant accumulation of ACs over time in GCs and not in the T cell zone, marginal zone and red pulp of the spleen in the absence of Mer-mediated clearance. In contrast, very low number

of TUNEL$^+$ cells were seen scattered over/in all areas of WT control spleen including GCs (Fig. 1C, left).

Tyro-3 and Axl expression was not compromised in Mer−/− mice

Axl, Mer and Tyro-3 are three members of a subfamily of receptors involved in the clearance of ACs (26, 27). While we show Mer expression on TBMϕs in GCs, the expression of Axl and Tyro-3 in GCs have never been examined. Given our current data showing long-term accumulation of ACs in Mer−/− GCs, we determined whether Axl and Tyro-3 were expressed on TBMϕs and whether Mer deficiency somehow altered the expression of these two receptors on TBMϕ in Mer−/− GCs. Spleen sections obtained from Mer−/− and WT control mice at d14 post-immunization were stained with either anti-Tyro-3 (2nd column, Fig. 2A) or anti-Axl (2nd column, Fig. 2B) in combination with PNA (1st column, Fig. 2A and B) and anti-CD68 (3rd column, Fig. 2A and B). We found that these two receptors were expressed on CD68$^+$ TBMϕs in GCs as evidenced by overlapped purple staining in overlay images (4th column, Fig. 2A and B) with no evident differences in expression between WT control and Mer−/− mice (Fig. 2). In a similar analysis, we also determined the expression of two other molecules (MFG-E8 and Tim-4) involved in phagocytosis and found no difference between WT and Mer−/− mice (data not shown). Together, these data indicate that accumulation of ACs in Mer−/− GCs is primarily due to Mer deficiency and not due to reduced expression of Axl, Tyro-3, MFG-E8 and Tim-4 in the absence of Mer.

Long-term accumulation of ACs in Mer−/− GCs led to enhanced long-lasting GC, AFC and IgG2 Ab responses

Next, we evaluated whether long-term accumulation of ACs in Mer−/− GCs led to elevated long-lasting GC, AFC and IgG2 Ab responses in Mer−/− mice. The anti-NP GC response in WT and Mer−/− mice was analyzed on days 21 and 80 post-first immunization. The GC response was examined by flow cytometric analysis where splenocytes from NP-OVA immunized mice were stained with GC B cell markers (B220, PNA and anti-Fas/CD95 Ab). We found significantly higher percentage of B220$^+$PNA^{hi}Fas^{hi} GC B cells in Mer−/− mice compared to WT controls on days 21 (Fig. 3A) and 80 (Fig. 3B). We also performed immunohistological analysis where spleen sections obtained from these mice on d21 and d80 post-immunization were stained with anti-IgD (blue) and PNA (red). Consistent with flow cytometry data, we found increased frequency of predominantly large GCs in Mer−/− mice on both days 21 (Fig. 3D) and 80 (Fig. 3F) compared to sparse and relatively smaller GCs in WT controls (Fig. 3C and E). Enhanced GC response and AC accumulation in GCs in Mer−/− mice also resulted in augmented NP-specific primary AFC response evaluated by ELISpot assay with splenocytes 21 days post-immunization (Fig. 3G and H). Long-lived IgG-producing AFCs in both spleen (Fig. 3I) and bone marrow (Fig. 3J) from Mer−/− mice (closed circle) were also significantly higher compared to WT controls (open circle) 80 days after NP-OVA immunization.

We extensively analyzed whether elevated long-term GC and AFC responses associated with accumulation of ACs in Mer−/− GCs translated to high titers of serum Abs in Mer−/− mice compared to WT controls over an extended period at multiple time points after NP-OVA immunization. The T cell dependent anti-NP response predominantly generates Abs of Th2 type IgG1 Abs in B6 mice (28). We found significantly higher titers of NP-specific total IgG (Fig. 4B) and IgG2 (Fig. 4D) Abs in Mer−/− mice compared to WT controls on days 21, 28, 45, 60 and 80 post-NP-OVA immunization with the peak response at day 60. This difference was also significant at d14 in the IgG2 titers (Fig. 4D). We did not observe any significant difference in anti-NP total IgM (Fig. 4A) and IgG1 (Fig. 4C) serum Ab levels. Due to the mixed background (B6 and 129) of Mer−/− and WT control mice where both

IgG2a (derived from 129 allele) and IgG2c (B6) can potentially be produced, we measured total IgG2 Ab levels (Fig. 4D). No significant difference was observed in IgG3 levels between Mer−/− and WT controls (data not shown).

We further analyzed affinity maturation of anti-NP serum IgG1 (Th2-biased) and IgG2 (Th1-biased) antibodies by ELISA from serum samples obtained from WT and Mer−/− mice on days 14, 21, 28, 45, 60 and 80 post-NP-OVA immunization. No significant differences in antigen affinity of both IgG1 and IgG2 Abs at any time point were revealed between WT and Mer−/− mice (data not shown).

Prolonged accumulation of ACs in Mer−/− GCs and enhanced AFC, GC and Ab responses led to high titers of ANAs

Even though delayed clearance of ACs is thought to contribute to ANA production in Mer−/− mice (3), the site where ACs may accumulate and influence ANA production in Mer−/− mice is not clear. To study the role of GC as a site of AC accumulation in Mer−/− mice which may lead to ANA production, we measured the titers of dsDNA-, histone- and nucleosome-specific Abs by ELISA in serum samples obtained from Mer−/− and WT control mice before (d0) and after (d28, d60, and d80) NP-OVA immunization. We observed significantly higher anti-dsDNA (Fig. 5A), anti-histone (Fig. 5B) and anti-nucleosome Abs (Fig. 5C) in Mer−/− mice (closed circle) compared to WT controls (open circle) on d28, d60 and d80 post-immunization while no significant difference in ANA titers was found between the two strains on d0 (Fig. 5). These ANA titers are in concordance with accumulation of ACs in GCs and enhanced GC, AFC and Ab responses in Mer−/− mice.

Elevated AFC, GC and IgG2 Ab responses in Mer−/− mice were due to increased activation and proliferation of B cells

Next, we evaluated whether the enhanced AFC, GC and IgG2 Ab responses apparently resulting from AC accumulation in Mer−/− GCs were due to increased activation of B cells in Mer−/− mice. Flow cytometric analysis of spleen cells obtained from Mer−/− and WT mice on d14 post-immunization revealed significantly higher percentage of activated B cells as evidenced by the expression of activation markers CD80 (left two panels, Fig. 6A) and CD86 (right two panels, Fig. 6A) in Mer−/− mice compared to WT controls. While we found no significant difference in $CD80^+$ cells between Mer−/− and control mice (left two panels, Fig. 6B) the percentage of $CD86^+$ cells remained significantly higher in Mer−/− mice compared to controls 21 days post-immunization (right two panels, Fig. 6B).

To study whether AC accumulation in GCs and elevated GC, AFC and IgG2 Ab responses in Mer−/− mice was due to increased B cell proliferation, we preformed an *in vivo* BrdU proliferation assay where we injected BrdU (i.p.) into Mer−/− and WT control mice 1–2 hr before harvesting spleens from these animals on d21 post-NP-OVA immunization. Immunohistological analysis was conducted on two consecutive spleen sections obtained from these mice. One was stained with anti-IgD (blue) and PNA (red) while the other one was stained with anti-IgD (blue) and anti-BrdU (brown, Fig. 6C). Both low (50x, left panels) and high (200x, right panels) magnification images are shown (Fig. 6C). We found significantly higher numbers of $BrdU^+$ cells in GCs and the red pulp areas of Mer−/− mice (bottom row, 2^{nd} and 4^{th} panels, Fig. 6C) compared to WT controls (upper row, 2^{nd} and 4^{th} panels, Fig. 6C). By performing a semi-quantitative analysis where we counted $BrdU^+$ cells in 45–50 representative GCs from seven mice of each genotype, we found the number of $BrdU^+$ cells in Mer−/− GCs (brown) to be significantly higher compared to WT controls (blue) (Fig. 6D).

Additionally, when we stained spleen sections from Mer−/− and control mice with GL7 (green) and Ki67 (red), a cell proliferation marker, we found analogous results as in Fig. 6C showing increased numbers of $Ki67^+$ cells in Mer−/− GCs (right two panels, Fig. 6E) compared to WT controls (left two panels, Fig. 6E).

Increased $CD4^+$ helper T cell responses in Mer−/− mice with elevated AFC, GC and IgG2 Ab responses

We observed an enhanced IgG2 Ab response in Mer−/− mice compared to WT controls (Fig. 4). Therefore, we analyzed whether AC accumulation in GCs and elevated GC, AFC and IgG2 Ab responses in Mer−/− mice were correlated with enhanced $CD4^+$ T helper cell activation and differentiation into effector cells including T_{FH} cells. Splenocytes obtained from Mer−/− and WT control mice 14 and 21 days post-immunization were stained with Abs against CD4, CD44, CD25 (IL-2Rα), CD62L, PD-1 and CXCR5. Flow cytometric analysis of stained spleen cells at both time points revealed significantly higher percentages of activated $CD4^+CD44^{hi}CD62L^{lo}$ short-lived (middle panels, Fig. 7A and B) and $CD4^+CD44^{hi}CD62L^{hi}$ memory (right panels, Fig. 7A and B) effector helper T cells in Mer−/− mice compared to WT controls.

Mer−/− mice also had increased percentages of $CD4^+CD25^+$ cells compared to WT controls on both d14 and 21 time points (left and middle panel, Fig. 7C and D). In addition, the expression of CD25 on $CD4^+$ cells were increased in Mer−/− mice compared to WT controls (shown in histograms overlay, right panels, Fig. 7C and D). This increased percentage of $CD4^+CD25^+$ cells in Mer−/− mice was associated with elevated $CD4^+PD\text{-}1^{hi}CXCR5^{hi}$ T_{FH} cells in Mer−/− mice compared to WT controls (Fig. 7E and F). We also evaluated the T_{FH} cell response in these mice 80 days post-immunization. $CD4^+PD\text{-}1^{hi}CXCR5^{hi}$ T_{FH} cell response in Mer−/− mice was on average three-fold higher compared to WT controls at d80 time point (Fig. 7G). We did not find any difference in $CD4^+CD25^+Foxp\text{-}3^+$ T regulatory (Treg) cells between these two strains at any time point (data not shown).

B cells and $CD4^+$ helper T cells from immunized Mer−/− mice proliferated at faster rate than WT control cells upon ex vivo stimulation

Using the BrdU proliferation assay we observed significantly higher number of proliferating B cells in Mer−/− GCs compared to WT controls (Fig. 6). To further delineate whether the microenvironment created in the GCs of Mer−/− mice intrinsically primed B and T cells to proliferate rapidly upon stimulation, we used an *ex vivo* cell proliferation assay for *in vivo* primed cells. MACS purified B cells obtained from Mer−/− and WT control mice 10 days post-NP-OVA immunization were labeled with CellTrace Violet followed by stimulation with anti-IgM and agonistic anti-CD40 Ab. By performing flow cytometric analysis we observed an increased rate of proliferation of B cells from Mer−/− mice compared to WT controls at both 72hr and 96hr post-stimulation as evident by the higher percentage of dividing B cells with lower CellTrace Violet intensity in Mer−/− mice (Fig. 8A). Similarly, we evaluated whether increased percentages of subsets of $CD4^+$ helper T cells (i.e., short-lived and memory effector cells as well as T_{FH} cells) in Mer−/− mice were due to enhanced proliferation of $CD4^+$ helper T cells in the presence of AC accumulation in GCs. MACS purified $CD4^+$ helper T cells from Mer−/− and WT control mice 10 days post-NP-OVA immunization were stained with CellTrace dye and then stimulated *ex vivo* with anti-CD3 and anti-CD28 Abs. The rate of proliferation of $CD4^+$ helper T cells was evaluated in a flow cytomteric analysis by determining the percentage of dividing cells. We found significantly higher percentage of cells in successive peaks with reduced CellTrace Violet fluorescence signifying more proliferating $CD4^+$ helper T cells in Mer−/− mice compared to WT controls at both 72hr and 96hr after stimulation (Fig. 8B).

CD4$^+$ helper T cells from immunized Mer−/− mice produced increased levels of Th1 and pro-inflammatory cytokines

We observed significantly higher Th1-biased IgG2 Abs in Mer−/− mice compared to WT controls. IgG2 Abs are believed to be driven by Th1 cytokines (i.e., IFN-γ). Therefore, we examined whether immunized Mer−/− mice had increased frequency of CD4$^+$IFN-γ$^+$ helper T cells. Splenocytes obtained from Mer−/− and control mice 10 and 15 days after NP-OVA immunization were stimulated *ex vivo* with PMA and Ionomycin. IFN-γ and IL-4 producing CD4$^+$ helper T cells were determined by intracellular staining with anti- IFN-γ and anti-IL-4 Abs through flow cytometry analysis at 0hr, 4hr and 8hr post-stimulation. We found that Mer−/− mice had significantly higher percentage of CD4$^+$IFN-γ$^+$ T cells compared to WT controls on both d10 (Fig. 9A, left panel) and d15 (Fig. 9B, left panel). We also observed increased frequency of CD4$^+$IL-4$^+$ T cells in Mer−/− mice compared to WT controls on d10 (Fig. 9A, right panel) but not on d15 (Fig. 9B, right panel) indicating an overall increase in both Th1 and Th2 responses at earlier time points.

We further determined levels of cytokines produced by CD4$^+$ helper T cells in Mer−/− mice. Purified T cells obtained from Mer−/− and WT control mice 10 days post NP-OVA-immunization were stimulated *ex vivo* with PMA and Ionomycin and supernatants were collected at 24hr and 48hr post-stimulation. Levels of cytokines were measured by flow cytometry using the BD™ Cytometric Bead Array (CBA) Th1/Th2/Th17 cytokine kit. Consistent with increased frequency of CD4$^+$IFN-γ$^+$ T cells in Mer−/− mice (Fig. 9A and B) CD4$^+$ helper T cells from Mer−/− mice produced significantly elevated levels of IFN-γ compared to WT controls at both 24hr and 48hr time points (Fig. 9C). In addition, we observed increased levels of TNF (both 24hr and 48hr) and IL-2 (24hr) in Mer−/− mice compared to WT controls (Fig. 9C). Albeit at low titers, levels of IL-6 and IL-17 (IL-17A) were also at least twofold higher in Mer−/− mice compared to WT controls at 24hr time point. Interestingly, we found significantly reduced IL-10 production in Mer−/− mice compared to WT controls (Fig. 9C). Finally, we observed similar levels of secreted IL-4 in both Mer−/− and control mice (data not shown).

Enhanced GC response and accumulation of ACs in Mer−/− GCs resulted in augmented memory B cell response in Mer−/− mice

GCs are microenvironments where B cells with high-affinity to foreign Ag are positively selected into memory B cells. We determined whether long-term accumulation of ACs in GCs and dysregulated GC response led to elevated memory B cell response in Mer−/− mice, which, in turn, may harbor autoreactive B cells. Mer−/− and WT control mice were immunized with NP-OVA as described earlier, rested for 80 days and then boosted (i.p.) with 50 μg of NP-OVA in PBS. Memory B cell response was indirectly evaluated by analyzing secondary AFCs 4 days after the boost. IgG-producing secondary AFCs in Mer−/− spleens (closed circle) were augmented compared to WT controls (open circle, Fig. 10A). These elevated secondary IgG AFC responses resulted in increased anamnestic anti-NP total IgG (Fig. 10B) and IgG2 (Fig. 10D) serum Ab titers in Mer−/− mice compared to WT controls. Analogous to the primary response, the secondary anti-NP IgG1 Ab responses remained comparable between Mer−/− and WT control mice (Fig. 10C).

Discussion

The development of autoimmunity in aged Mer−/− mice is attributed to delayed clearance of ACs over time (3). However, the site where delayed clearance of ACs may occur in Mer−/− mice and alter B cell tolerance leading to ANA production is unclear. Since many B cells undergo apoptotic cell death in GCs due to clonal selection as a function of GC homeostasis, we propose that GCs are the primary site where ACs accumulate in the absence of Mer-

mediated clearance. Consistent with this idea, we recently showed that ACs accumulate in GCs in the absence of Mer by analyzing the early (d14) GC response against the TD Ag NP-CGG (6).

While we previously showed AC accumulation in GCs and the enhanced AFC, GC and IgG2 Ab responses in Mer−/− mice at earlier time point (6), it was not clear whether ACs continue to accumulate over time even in the presence of several other receptors and molecules (i.e, Axl, Tyro-3, MFG-E8, Tim-4, C1q and CD36) which may clear dead and/or dying cells from GCs at later time points after the initial peak GC response wanes. This is particularly important to study because long-term accumulation of ACs in GCs in Mer−/− mice in the presence of other phagocytic receptors can further highlight the significant role played by Mer in clearing ACs in GCs and have major implications in breaking B cell tolerance leading to ANA production in Mer−/− mice. Our analysis of the later time points (up to 80 days) indeed revealed long-term AC accumulation in GCs leading to steady state elevated AFC, GC and IgG2 Ab responses in Mer−/− mice compared to WT controls. These elevated responses and AC accumulation in Mer−/− GCs were tightly linked to significantly higher titers of ANAs in Mer−/− mice compared to WT controls, indicating a break in peripheral B cell tolerance due to delayed clearance of ACs in GCs. This is the first report to show the effect of long-term AC accumulation in GCs on ANA production in Mer−/− mice.

The enhanced AFC, GC and IgG2 Ab responses in Mer−/− mice in our studies were a result of significantly increased activation and proliferation of total and GC B cells, T cells and greater numbers of activated effector $CD4^+$ helper T cells including T_{FH} cells. The increased frequency of GC B cells and effector helper T cells in Mer−/− mice was also associated with significantly elevated long-lived primary and memory responses compared to WT controls. We did not, however, observe any differences in affinity-maturation of both Th2/IgG1 and Th1/IgG2 Ab responses between WT control and Mer−/− mice. Importantly, we ruled out the contribution of the potentially reduced expression of several other bridging molecules/receptors (i.e., Axl, Tyro-3, MFG-E8 and Tim-4) to AC accumulation in Mer−/− GCs. These data demonstrate that accumulation of ACs in Mer−/− GCs is primarily due to a deficiency in Mer expression and not due to altered expression of Axl, Tyro-3, MFG-E8 and Tim-4, potentially induced by Mer deficiency.

We observed enhanced long lasting AFC, GC and IgG2 Ab responses in Mer−/− mice compared to WT controls. In contrast, the Cohen group previously reported no difference in T-dependent Ab responses between Mer−/− and control mice by measuring only serum OVA-specific total IgG and IgG1 (Th2) Ab titers 14 days after immunizing these mice with OVA (23). The same group in a more recent publication showed decreased GC response in Mer−/− mice in response to chronic graft-versus-host response mediated by allogenic bm12 cells transferred into Mer−/− mice (29). While both these reports by the Cohen group used different models to determine the role of Mer in regulating MZ B cell response and tolerance (23, 29) these data may not be extrapolated to assign a role for Mer-mediated clearance of ACs from GCs in regulating follicular GC B cell and Ab responses against various T-dependent Ags. Our results at d14 (Fig. 3B, C) are analogous to the data published by the Cohen group where they reported no differences in total OVA-specific IgG1 Ab titers between WT control and Mer−/− mice 14 days after immunization (23). However, when we measured serum Ab titers at multiple later time points over a period of 80 days post-NP-OVA immunization, we observed significantly higher total NP-specific IgG titers in Mer−/− mice compared to WT controls starting from day 21 through day 80. Th1-biased IgG2 Ab response was significantly higher in Mer−/− mice compared to WT controls starting from day 14 through day 80 while Th2-IgG1 response remained similar between the two strains during this period, indicating enhanced steady state Th1 cytokine driven IgG2 Ab responses in Mer−/− mice in the presence of AC accumulation in GCs.

In the absence of efficient removal of ACs, uncleared ACs in Mer−/− GCs can undergo necrotic cell death (termed secondary necrosis) allowing the rupture of cellular membranes and release of danger associated molecular patterns (DAMPs) (30, 31). DAMPs released from these cells can then stimulate both phagocytes (i.e., TBMϕs) and B cells via intracellular or extracellular DAMP receptors (DAMP-Rs) such as Toll-like and NOD-like receptors expressed by these cells. The pro-inflammatory conditions generated through DAMP-R stimulation of TBMϕs and B cells may drive differentiation of helper T cells towards Th1and may lead to a break in T cell tolerance. Consistent with this idea, we find increased levels of Th1 (i.e., IFN-γ and IL-2) and pro-inflammatory (i.e., TNF and IL-6) cytokines in Mer−/− $CD4^+$ helper T cells compared to WT controls. Mer−/− mice also have a defect in AC clearance in the thymus (32), which may give rise to autoreactive T cells. Subsequently, abnormal help from GC T_{FH} cells could facilitate enhanced GC B cell responses and the process of breaking B cell tolerance. The evidence of loss of AC-induced T cell tolerance in the absence of Mer was previously described (33). In accordance with our results, a potential role for defective T_{FH} cell compartment in breaking GC tolerance and promoting autoimmunity has also been described in a number of autoimmune mouse models including *Roquin*$^{san/san}$ (*sanroque*) (34) and BXSB.*yaa* mice (35, 36).

An increasing body of evidence from literature suggests that a failure to clear ACs results in autoimmunity (2–5, 37–39). In addition to Mer and MFG-E8 deficiency, mice deficient in several other molecules involved in the phagocytosis and clearance of ACs such as C1q (C1q−/−) and Tim-4 (Tim-4−/−) all developed autoimmunity (4, 5). Syngeneic AC administration or blocking of phosphatidylserine-mediated phagocytosis of ACs results in the production of ANAs and IgG deposition on kidney glomeruli (40, 41). Impaired phagocytosis of ACs by peritoneal macrophages from autoimmune-prone mice has been described (42, 43). Macrophages from human SLE (systemic lupus erythematosus) patients have a defect in phagoytosis of ACs (37–39). SLE patients and lupus-prone (SWR x NZB) F1 mice had a marked increase in the frequency of peripheral lymphocyte apoptosis (44–46). These data clearly indicate that a defect in AC clearance or increased rate of apoptosis can both potentially contribute to AC accumulation and loss of immune regulation. Our data from the present study suggest that GCs are the primary site where ACs accumulated in the absence of Mer-meditated clearance. This AC accumulation in Mer−/− GCs appears to be due to a defect in AC clearance and not to increased apoptosis of B cells in Mer−/− GCs (T.N.K and Z.S.M.R, unpublished data).

Our data present evidence for prolonged accumulation of ACs in GCs in the absence of Mer that leads to enhanced AFC, GC and Th1-IgG2 Ab responses. Consistent with elevated Th1-IgG2 Ab responses, we find increased activation, proliferation and secretion of Th1 cytokines (i.e., IL-2, TNF and IFN-γ) especially IFN-γ by $CD4^+$ helper T cells from immunized Mer−/− mice compared to WT controls (Fig. 9). These data are in agreement with previous studies showing elevated mRNA levels of the Th1- cytokine IFN-γ in the lymphoid organs of aged triple receptor tyrosine kinase knock out (Tyro3−/−, Axl−/− and Mer−/−) mice (47). Recently, Ye et al. showed that retinal self-Ag induced a predominant Th1 effector response including increased levels of IFN-γ production and higher frequency of IFN-γ^+ $CD4^+$ helper T cells (48). The Th1/IFN-γ/IgG2a response is associated with lupus-like disease in mice (49, 50). 3H9.Mer$^{-/-}$ mice also spontaneously produced IgG2c (an isoform of IgG2a) anti-DNA Abs (23). These reports together suggested a possible role for Th1 lineage differentiation in enhancing AFC, GC and IgG2a/c Ab responses in these mice. In the light of these previous studies and our current observations, a key role for GCs can be proposed where defective clearance of ACs from GCs leads to dysregulated B and T cell functions and helps break B cell tolerance leading to the development of enhanced IgG2a/c Abs specific for either foreign or self-Ags in Mer−/− mice. Consistent with this notion we observed high titers of ANAs in NP-OVA immunized Mer−/− mice in the

presence of continued AC accumulation in GCs over time compared to WT controls. Delayed clearance of ACs in GCs and anti-nuclear Ab production were also observed in MFG-E8−/− mice (2, 8). Together, these data indicate that clearance of ACs in GCs may play a pivotal role in regulating signals required for optimal B and T cell responses in the periphery and that failed or defective clearance of ACs in GCs may provide altered signaling leading to dysregulation of GC homeostasis and functions which may contribute to a break in peripheral immune tolerance and induction of autoimmunity.

Acknowledgments

These studies were supported by a grant from the NIH to Z.S.M.R. (AI091670)

We thank Drs. Cathie Calkins and Chris Snyder from Thomas Jefferson University for their critical reading of the manuscript and constructive comments.

Abbreviations

MerTK	Mer receptor tyrosine kinase
GC	germinal center
AFC	antibody forming cell
TBMϕ	tingible body macrophage
DC	dendritic cell
AC	apoptotic cell
MZ	marginal zone
TD-Ag	T cell dependent-Ag
NP-OVA	(4-hydroxy-3-nitrophenyl) acetyl $(NP)_{16}$-ovalbumin (OVA)
T_{FH}	T follicular helper cell
ANA	anti-nuclear antibody

References

1. Ravichandran KS, Lorenz U. Engulfment of apoptotic cells: signals for a good meal. Nat Rev Immunol. 2007; 7:964–974. [PubMed: 18037898]
2. Hanayama R, Tanaka M, Miyasaka K, Aozasa K, Koike M, Uchiyama Y, Nagata S. Autoimmune disease and impaired uptake of apoptotic cells in MFG-E8-deficient mice. Science. 2004; 304:1147–1150. [PubMed: 15155946]
3. Cohen PL, Caricchio R, Abraham V, Camenisch TD, Jennette JC, Roubey RA, Earp HS, Matsushima G, Reap EA. Delayed apoptotic cell clearance and lupus-like autoimmunity in mice lacking the c-mer membrane tyrosine kinase. J Exp Med. 2002; 196:135–140. [PubMed: 12093878]
4. Rodriguez-Manzanet R, Sanjuan MA, Wu HY, Quintana FJ, Xiao S, Anderson AC, Weiner HL, Green DR, Kuchroo VK. T and B cell hyperactivity and autoimmunity associated with niche-specific defects in apoptotic body clearance in TIM-4-deficient mice. Proc Natl Acad Sci U S A. 2010; 107:8706–8711. [PubMed: 20368430]
5. Botto M, Dell'Agnola C, Bygrave AE, Thompson EM, Cook HT, Petry F, Loos M, Pandolfi PP, Walport MJ. Homozygous C1q deficiency causes glomerulonephritis associated with multiple apoptotic bodies. Nat Genet. 1998; 19:56–59. [PubMed: 9590289]
6. Rahman ZS, Shao WH, Khan TN, Zhen Y, Cohen PL. Impaired apoptotic cell clearance in the germinal center by Mer-deficient tingible body macrophages leads to enhanced antibody-forming cell and germinal center responses. J Immunol. 2010; 185:5859–5868. [PubMed: 20952679]

7. Smith JP, Burton GF, Tew JG, Szakal AK. Tingible body macrophages in regulation of germinal center reactions. Dev Immunol. 1998; 6:285–294. [PubMed: 9814602]
8. Kranich J, Krautler NJ, Heinen E, Polymenidou M, Bridel C, Schildknecht A, Huber C, Kosco-Vilbois MH, Zinkernagel R, Miele G, Aguzzi A. Follicular dendritic cells control engulfment of apoptotic bodies by secreting Mfge8. J Exp Med. 2008; 205:1293–1302. [PubMed: 18490487]
9. Voll RE, Herrmann M, Roth EA, Stach C, Kalden JR, Girkontaite I. Immunosuppressive effects of apoptotic cells. Nature. 1997; 390:350–351. [PubMed: 9389474]
10. Savill J, Dransfield I, Gregory C, Haslett C. A blast from the past: clearance of apoptotic cells regulates immune responses. Nat Rev Immunol. 2002; 2:965–975. [PubMed: 12461569]
11. McGaha TL, Chen Y, Ravishankar B, van Rooijen N, Karlsson MC. Marginal zone macrophages suppress innate and adaptive immunity to apoptotic cells in the spleen. Blood. 2011; 117:5403–5412. [PubMed: 21444914]
12. Ravishankar B, Liu H, Shinde R, Chandler P, Baban B, Tanaka M, Munn DH, Mellor AL, Karlsson MC, McGaha TL. Tolerance to apoptotic cells is regulated by indoleamine 2,3-dioxygenase. Proc Natl Acad Sci U S A. 2012; 109:3909–3914. [PubMed: 22355111]
13. Fadok VA, Warner ML, Bratton DL, Henson PM. CD36 is required for phagocytosis of apoptotic cells by human macrophages that use either a phosphatidylserine receptor or the vitronectin receptor (alpha v beta 3). J Immunol. 1998; 161:6250–6257. [PubMed: 9834113]
14. Nagata S, Hanayama R, Kawane K. Autoimmunity and the clearance of dead cells. Cell. 2010; 140:619–630. [PubMed: 20211132]
15. Miyanishi M, Tada K, Koike M, Uchiyama Y, Kitamura T, Nagata S. Identification of Tim4 as a phosphatidylserine receptor. Nature. 2007; 450:435–439. [PubMed: 17960135]
16. Lemke G, Rothlin CV. Immunobiology of the TAM receptors. Nat Rev Immunol. 2008; 8:327–336. [PubMed: 18421305]
17. Linger RM, Keating AK, Earp HS, Graham DK. TAM receptor tyrosine kinases: biologic functions, signaling, and potential therapeutic targeting in human cancer. Adv Cancer Res. 2008; 100:35–83. [PubMed: 18620092]
18. Shao WH, Zhen Y, Eisenberg RA, Cohen PL. The Mer receptor tyrosine kinase is expressed on discrete macrophage subpopulations and mainly uses Gas6 as its ligand for uptake of apoptotic cells. Clin Immunol. 2009; 133:138–144. [PubMed: 19631584]
19. Hanayama R, Tanaka M, Miwa K, Shinohara A, Iwamatsu A, Nagata S. Identification of a factor that links apoptotic cells to phagocytes. Nature. 2002; 417:182–187. [PubMed: 12000961]
20. D'Cruz PM, Yasumura D, Weir J, Matthes MT, Abderrahim H, LaVail MM, Vollrath D. Mutation of the receptor tyrosine kinase gene Mertk in the retinal dystrophic RCS rat. Hum Mol Genet. 2000; 9:645–651. [PubMed: 10699188]
21. Savill J, Fadok V. Corpse clearance defines the meaning of cell death. Nature. 2000; 407:784–788. [PubMed: 11048729]
22. Rothlin CV, Ghosh S, Zuniga EI, Oldstone MB, Lemke G. TAM receptors are pleiotropic inhibitors of the innate immune response. Cell. 2007; 131:1124–1136. [PubMed: 18083102]
23. Shao WH, Kuan AP, Wang C, Abraham V, Waldman MA, Vogelgesang A, Wittenburg G, Choudhury A, Tsao PY, Miwa T, Eisenberg RA, Cohen PL. Disrupted Mer receptor tyrosine kinase expression leads to enhanced MZ B-cell responses. J Autoimmun. 2010; 35:368–374. [PubMed: 20822883]
24. Rahman ZSM, Rao SP, Kalled SL, Manser T. Normal Induction but Attenuated Progression of Germinal Center Responses in BAFF and BAFF-R Signaling-Deficient Mice. Journal of Experimental Medicine. 2003; 198:1157–1169. [PubMed: 14557413]
25. Vora KA, Tumas-Brundage KM, Lentz VM, Cranston A, Fishel R, Manser T. Severe attenuation of the B cell immune response in Msh2-deficient mice. J Exp Med. 1999; 189:471–482. [PubMed: 9927509]
26. Lemke G, Rothlin CV. Immunobiology of the TAM receptors. Nat Rev Immunol. 2008; 8:327–336. [PubMed: 18421305]
27. Seitz HM, Camenisch TD, Lemke G, Earp HS, Matsushima GK. Macrophages and dendritic cells use different Axl/Mertk/Tyro3 receptors in clearance of apoptotic cells. J Immunol. 2007; 178:5635–5642. [PubMed: 17442946]

28. Lalor PA, Nossal GJ, Sanderson RD, McHeyzer-Williams MG. Functional and molecular characterization of single, (4-hydroxy-3-nitrophenyl)acetyl (NP)-specific, IgG1+ B cells from antibody-secreting and memory B cell pathways in the C57BL/6 immune response to NP. Eur J Immunol. 1992; 22:3001–3011. [PubMed: 1425924]
29. Shao WH, Zhen Y, Finkelman FD, Eisenberg RA, Cohen PL. Intrinsic unresponsiveness of Mertk(−/−) B cells to chronic graft-versus-host disease is associated with unmodulated CD1d expression. J Autoimmun. 2012
30. Kono H, Rock KL. How dying cells alert the immune system to danger. Nat Rev Immunol. 2008; 8:279–289. [PubMed: 18340345]
31. Chen GY, Nunez G. Sterile inflammation: sensing and reacting to damage. Nat Rev Immunol. 2010; 10:826–837. [PubMed: 21088683]
32. Scott RS, McMahon EJ, Pop SM, Reap EA, Caricchio R, Cohen PL, Earp HS, Matsushima GK. Phagocytosis and clearance of apoptotic cells is mediated by MER. Nature. 2001; 411:207–211. [PubMed: 11346799]
33. Wallet MA, Sen P, Flores RR, Wang Y, Yi Z, Huang Y, Mathews CE, Earp HS, Matsushima G, Wang B, Tisch R. MerTK is required for apoptotic cell-induced T cell tolerance. J Exp Med. 2008; 205:219–232. [PubMed: 18195070]
34. Linterman MA, Rigby RJ, Wong RK, Yu D, Brink R, Cannons JL, Schwartzberg PL, Cook MC, Walters GD, Vinuesa CG. Follicular helper T cells are required for systemic autoimmunity. J Exp Med. 2009; 206:561–576. [PubMed: 19221396]
35. Craft JE. Follicular helper T cells in immunity and systemic autoimmunity. Nat Rev Rheumatol. 2012; 8:337–347. [PubMed: 22549246]
36. Bubier JA, Sproule TJ, Foreman O, Spolski R, Shaffer DJ, Morse HC 3rd, Leonard WJ, Roopenian DC. A critical role for IL-21 receptor signaling in the pathogenesis of systemic lupus erythematosus in BXSB-Yaa mice. Proc Natl Acad Sci U S A. 2009; 106:1518–1523. [PubMed: 19164519]
37. Gaipl US, Munoz LE, Grossmayer G, Lauber K, Franz S, Sarter K, Voll RE, Winkler T, Kuhn A, Kalden J, Kern P, Herrmann M. Clearance deficiency and systemic lupus erythematosus (SLE). J Autoimmun. 2007; 28:114–121. [PubMed: 17368845]
38. Baumann I, Kolowos W, Voll RE, Manger B, Gaipl U, Neuhuber WL, Kirchner T, Kalden JR, Herrmann M. Impaired uptake of apoptotic cells into tingible body macrophages in germinal centers of patients with systemic lupus erythematosus. Arthritis Rheum. 2002; 46:191–201. [PubMed: 11817590]
39. Ren Y, Tang J, Mok MY, Chan AW, Wu A, Lau CS. Increased apoptotic neutrophils and macrophages and impaired macrophage phagocytic clearance of apoptotic neutrophils in systemic lupus erythematosus. Arthritis Rheum. 2003; 48:2888–2897. [PubMed: 14558095]
40. Asano K, Miwa M, Miwa K, Hanayama R, Nagase H, Nagata S, Tanaka M. Masking of phosphatidylserine inhibits apoptotic cell engulfment and induces autoantibody production in mice. J Exp Med. 2004; 200:459–467. [PubMed: 15302904]
41. Mevorach D, Zhou JL, Song X, Elkon KB. Systemic exposure to irradiated apoptotic cells induces autoantibody production. J Exp Med. 1998; 188:387–392. [PubMed: 9670050]
42. Potter PK, Cortes-Hernandez J, Quartier P, Botto M, Walport MJ. Lupus-prone mice have an abnormal response to thioglycolate and an impaired clearance of apoptotic cells. J Immunol. 2003; 170:3223–3232. [PubMed: 12626581]
43. Licht R, Dieker JW, Jacobs CW, Tax WJ, Berden JH. Decreased phagocytosis of apoptotic cells in diseased SLE mice. J Autoimmun. 2004; 22:139–145. [PubMed: 14987742]
44. Lorenz HM, Grunke M, Hieronymus T, Herrmann M, Kuhnel A, Manger B, Kalden JR. In vitro apoptosis and expression of apoptosis-related molecules in lymphocytes from patients with systemic lupus erythematosus and other autoimmune diseases. Arthritis Rheum. 1997; 40:306–317. [PubMed: 9041943]
45. Emlen W, Niebur J, Kadera R. Accelerated in vitro apoptosis of lymphocytes from patients with systemic lupus erythematosus. J Immunol. 1994; 152:3685–3692. [PubMed: 8144943]

46. Kalled SL, Cutler AH, Burkly LC. Apoptosis and altered dendritic cell homeostasis in lupus nephritis are limited by anti-CD154 treatment. J Immunol. 2001; 167:1740–1747. [PubMed: 11466399]

47. Lu Q, Lemke G. Homeostatic regulation of the immune system by receptor tyrosine kinases of the Tyro 3 family. Science. 2001; 293:306–311. [PubMed: 11452127]

48. Ye F, Han L, Lu Q, Dong W, Chen Z, Shao H, Kaplan HJ, Li Q, Lu Q. Retinal self-antigen induces a predominantly Th1 effector response in Axl and Mertk double-knockout mice. J Immunol. 2011; 187:4178–4186. [PubMed: 21918185]

49. Takahashi S, Fossati L, Iwamoto M, Merino R, Motta R, Kobayakawa T, Izui S. Imbalance towards Th1 predominance is associated with acceleration of lupus-like autoimmune syndrome in MRL mice. J Clin Invest. 1996; 97:1597–1604. [PubMed: 8601623]

50. Ehlers M, Fukuyama H, McGaha TL, Aderem A, Ravetch JV. TLR9/MyD88 signaling is required for class switching to pathogenic IgG2a and 2b autoantibodies in SLE. J Exp Med. 2006; 203:553–561. [PubMed: 16492804]

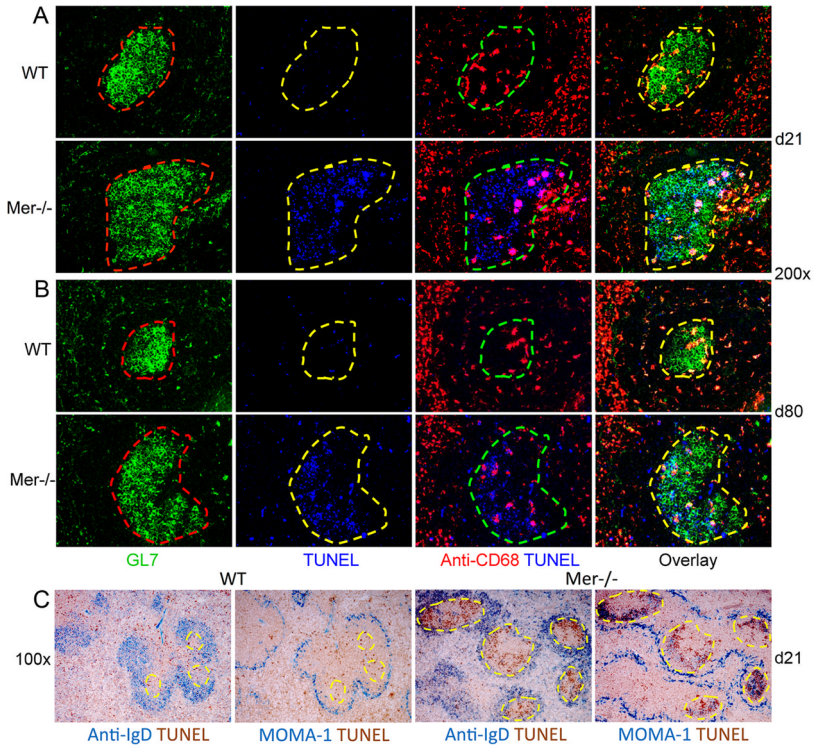

Figure 1. TUNEL$^+$ apoptotic cells accumulate predominantly in GCs and not in the marginal zone, T cell zone or red pulp in the spleen of Mer−/− mice

Immunohistology was performed on spleen tissue obtained on day 21 (A) and 80 (B) post-NP-OVA immunization of WT and Mer−/− mice. Spleen sections were stained with GL7 (green, 1st column), TUNEL (blue, 2nd column) and anti-CD68 (red, 3rd column). In the 1st column, the GC areas shown in dotted red lines were defined by the presence of GL7$^+$ cells (green). These GC areas were carried over to subsequent panels to show TUNEL$^+$ (2nd column) cells within GCs. Two (TUNEL and anti-CD68) and three (GL7, TUNEL and anti-CD68) color overlay images are shown in the 3rd and 4th columns, respectively. (C) One of two consecutive spleen sections obtained from WT control (left panels) and Mer−/− (right panels) mice was stained with anti-IgD (blue) and TUNEL (brown). The other section was stained with MOMA-1 (blue) and TUNEL (brown). Original magnification of images was 200x for (A and B) and 100x for (C). GC areas are shown in dotted yellow lines in (C). These data represent age- and sex-matched seven to eight mice of each genotype for each time point.

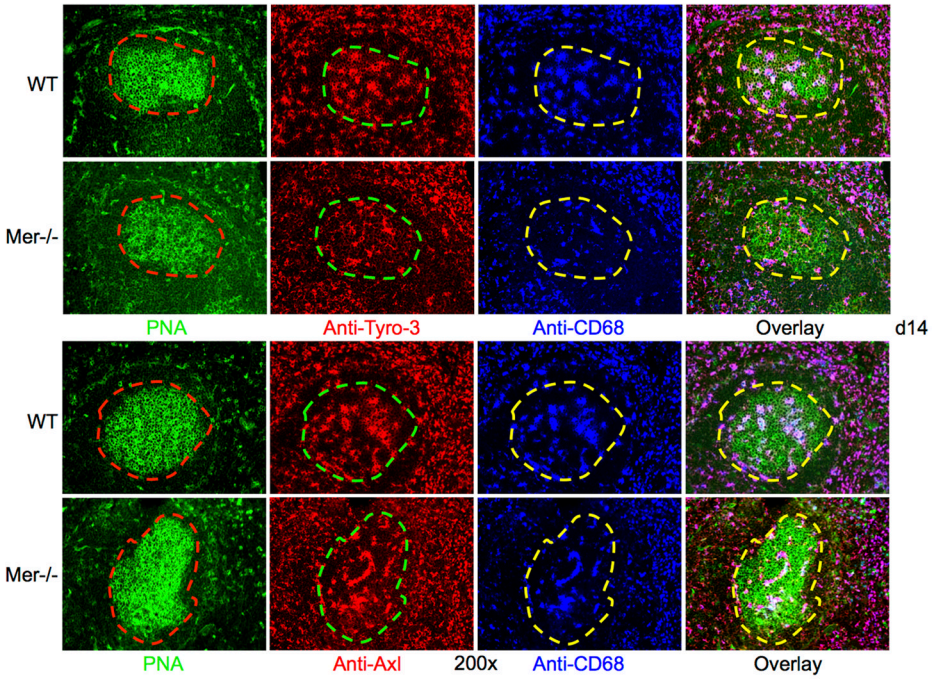

Figure 2. Mer deficiency does not lead to reduced expression of Tyro-3 and Axl

(A) Three-color immunohistological analysis was performed on spleen tissue obtained from WT (upper row) and Mer−/− (lower row) mice 14 days after immunization. Spleen sections were co-stained with PNA (green), anti-Tyro-3 (red) and anti-CD68 (blue). In the 1st column, the GC areas shown in dotted red lines were defined by the presence of PNA^{+} cells (green). These GC areas were carried over to subsequent panels to show anti-Tyro-3^{+} (2nd column) and CD68^{+} (3rd column) TBMϕs within GCs. Three color overlay images are shown in the 4th column. (B) Identical analysis as in (A) was carried out where anti-Tyro-3 staining was replaced by anti-Axl. These data were generated from seven age- and sex-matched WT and Mer−/− mice each.

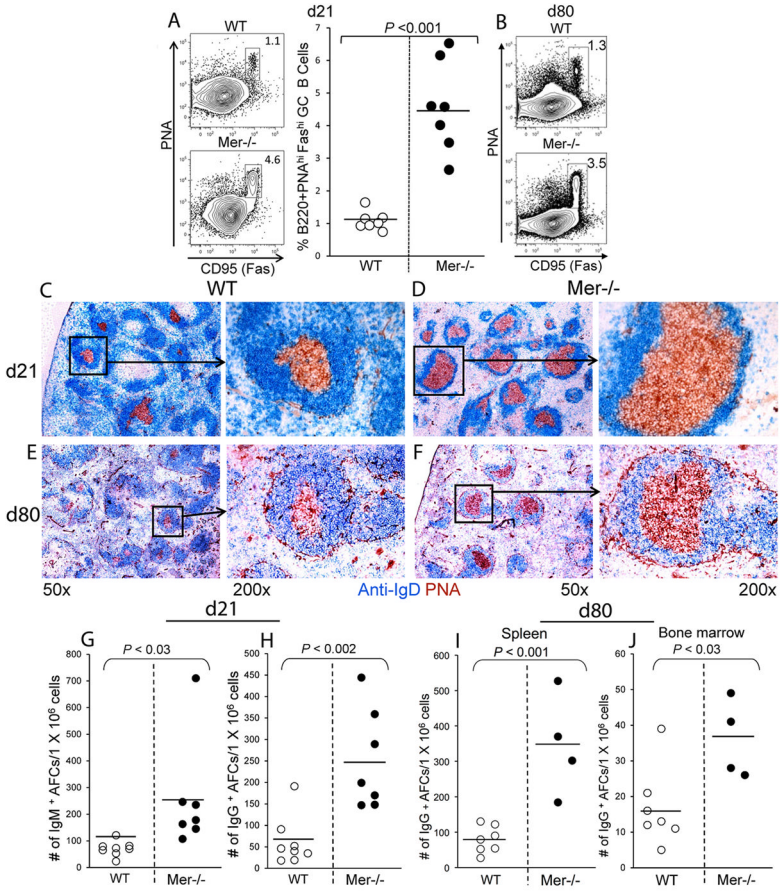

Figure 3. Augmented primary GC and AFC responses in the absence of Mer over time

Flow cytometric analysis was performed on splenocytes obtained from WT and Mer−/− mice on days 21 (A) and 80 (B) post-immunization with NP-OVA. Splenocytes were stained with GC B cell markers (B220, PNA and anti-CD95/Fas). Representative contour plots obtained from WT (upper panel) and Mer−/− (lower panel) mice on d21 show $B220^{+}PNA^{hi}Fas^{hi}$ GC B cells in rectangular gates (A, left panel). The percentage of $B220^{+}PNA^{hi}Fas^{hi}$ GC B cells in WT (open circle) and Mer−/− (closed circle) mice is shown in scatter plots (A, right panel). Analysis of samples obtained on day21 was performed on individual mice and on day 80 was performed on pooled samples of seven WT control (top) and four Mer−/− (bottom) mice where $B220^{+}PNA^{hi}Fas^{hi}$ GC B cells are shown in rectangular gates only (B). Spleen sections obtained from WT (C and E) and Mer−/− mice (D and F) on days 21 and 80 post-NP-OVA immunization were stained with anti-IgD (blue) and PNA (red). Low (50x) and high magnification (200x) representative images are shown. The number of short-lived splenic NP-specific IgM (G) and IgG (H) secreting AFCs were measured by ELISpot at indicated days after immunization of WT (open circle) and Mer−/− (closed circle) mice with NP-OVA. The number of long-lived splenic (I) and bone marrow-derived (J) NP-specific IgG-producing AFCs were measured by ELISpot 80 days post-immunization. Each circle represents the number of AFCs per 1×10^{6} splenocytes obtained from an individual mouse. Horizontal bars represent the mean values. These data were obtained from age- and sex-matched four to seven mice per genotype.

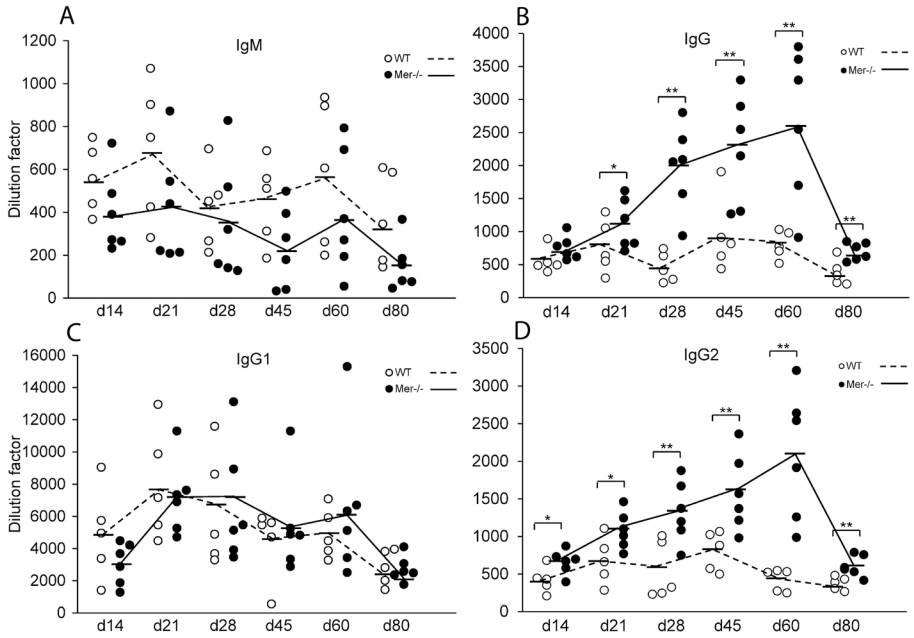

Figure 4. Augmented IgG and IgG2 Ab responses in Mer−/− mice

Anti-NP IgM (A), IgG (B), IgG1 (C) and IgG2 (D) Ab titers were measured by ELISA in WT (open circle) and Mer−/− (closed circle) serum samples obtained on multiple time points (days 14, 21, 28, 45, 60 and 80) post-immunization of these mice with NP-OVA. The dashed lines represent WT and solid lines represent Mer−/− mice. Each circle represents an individual mouse and horizontal bars represent the mean values. *P* values of <0.05 and <0.01 are depicted as * and **, respectively. These data were obtained from age- and sex-matched five to six mice of each genotype at each time point.

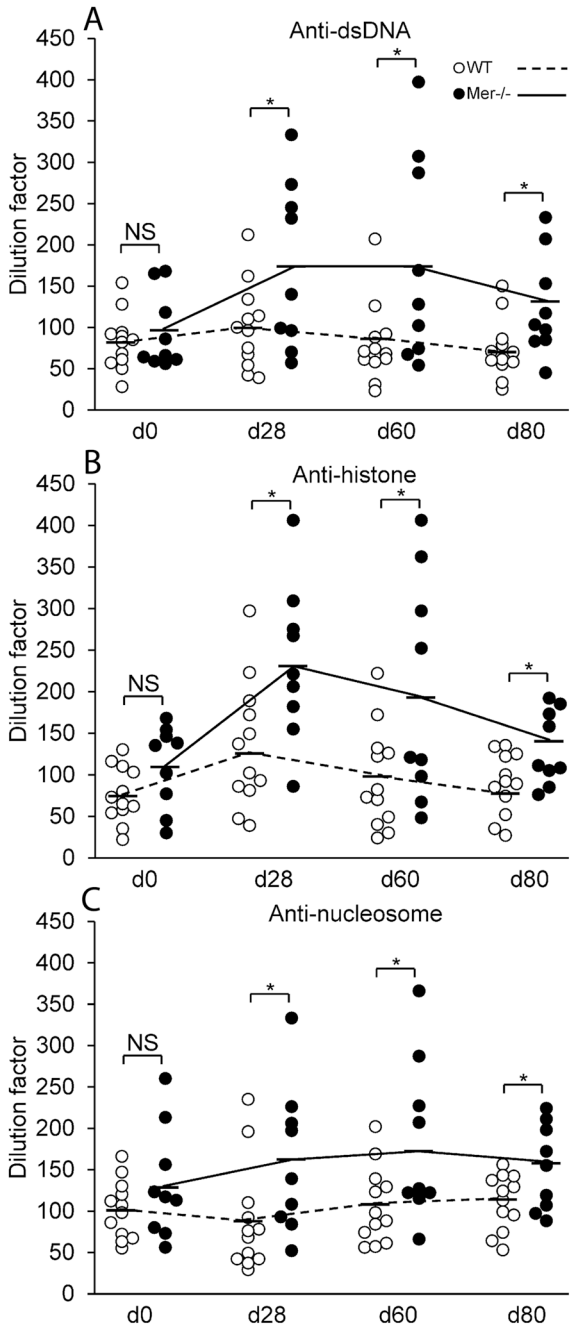

Figure 5. High titers of ANAs in NP-OVA immunized Mer−/− mice

Anti-dsDNA (A), anti-histone (B) and anti-nucleosome (C) Abs were measured by ELISA in serum samples obtained from WT (open circle, n =12) and Mer−/− (closed circle, n = 9) mice on multiple time points before (d0) and after (d28, d60 and d80) immunization with NP-OVA. The dashed lines represent WT and solid lines represent Mer−/− mice. Each circle represents one individual mouse and bars represent the mean values. P values of <0.05 are depicted as *, NS= Not Significant.

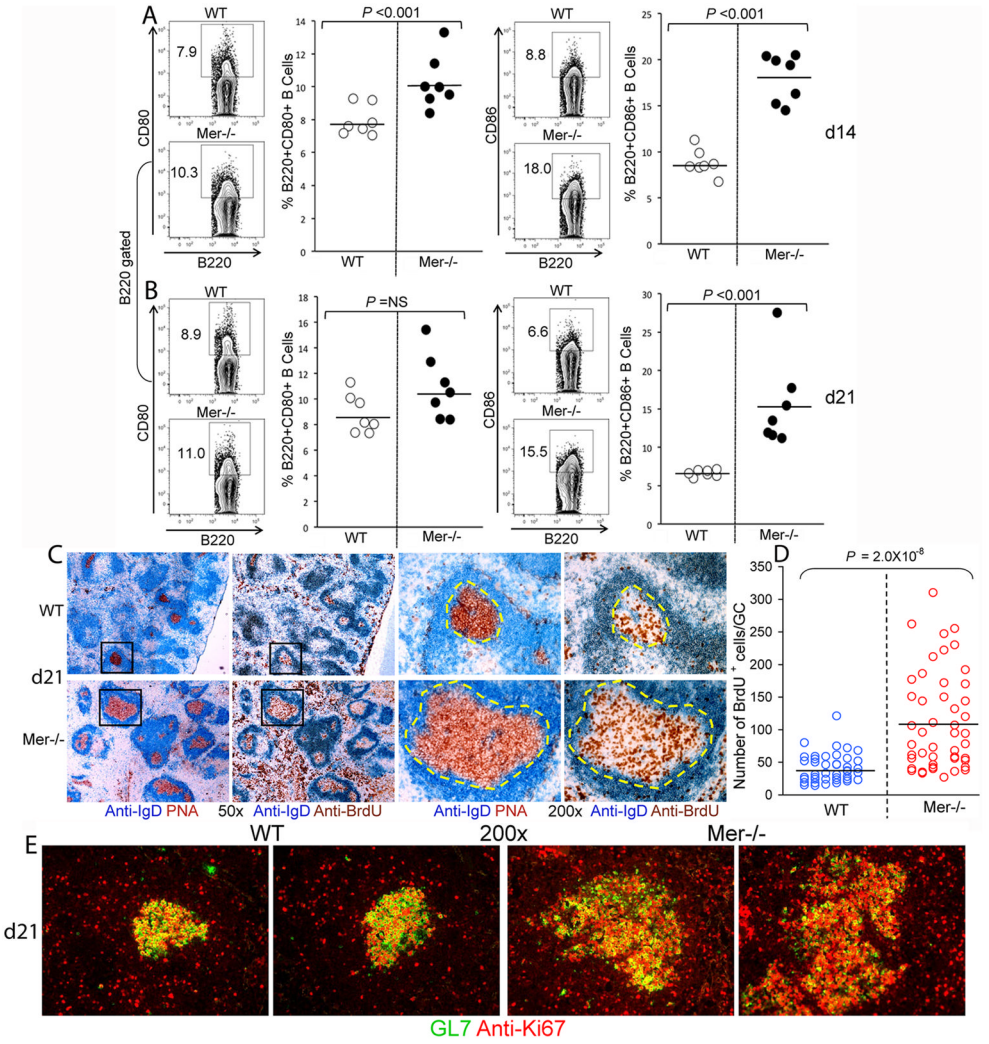

Figure 6. Increased percentage of activated and proliferating B cells in Mer−/− mice

B cell activation was evaluated by flow cytometric analysis of spleen cells obtained at days 14 (A) and 21 (B) post-immunization of WT and Mer−/− mice with NP-OVA. Spleen cells were stained with antibodies against B cell activation markers CD80 (A and B, left two panels) and CD86 (A and B, right two panels). The percentage of $B220^{+}CD80^{+}$ (left panels) and $B220^{+}CD86^{+}$ (right panels) cells in WT (open circle) and Mer−/− (closed circle) mice is shown in scatter plots. (C) Immunohistological analysis was performed on two consecutive spleen sections obtained from WT (upper row) and Mer−/− (lower row) mice on day 21 after NP-OVA immunization. One section (1st and 3rd columns) was stained using anti-IgD (blue) and PNA (red) and the other (2nd and 4th columns) was stained with anti-IgD (blue) and anti-BrdU (brown). The high magnification (200x) images shown in 3rd and 4th columns are obtained from low magnification (50x) GCs delineated by rectangles in the 1st and 2nd columns. (D) Semi-quantitative analysis of $BrdU^{+}$ B cells per GC was performed by counting $BrdU^{+}$ cells in 45–50 representative GCs from seven WT (blue) and eight Mer−/− mice. (E): Spleen sections obtained from WT (left two panels) and Mer−/− (right two panels) mice on day 21 after NP-OVA immunization were stained with GL7 (green) and anti-Ki67 (red). Original magnification of images was 200x. Two representative images from each strain are shown. These data represent at least seven mice of each genotype.

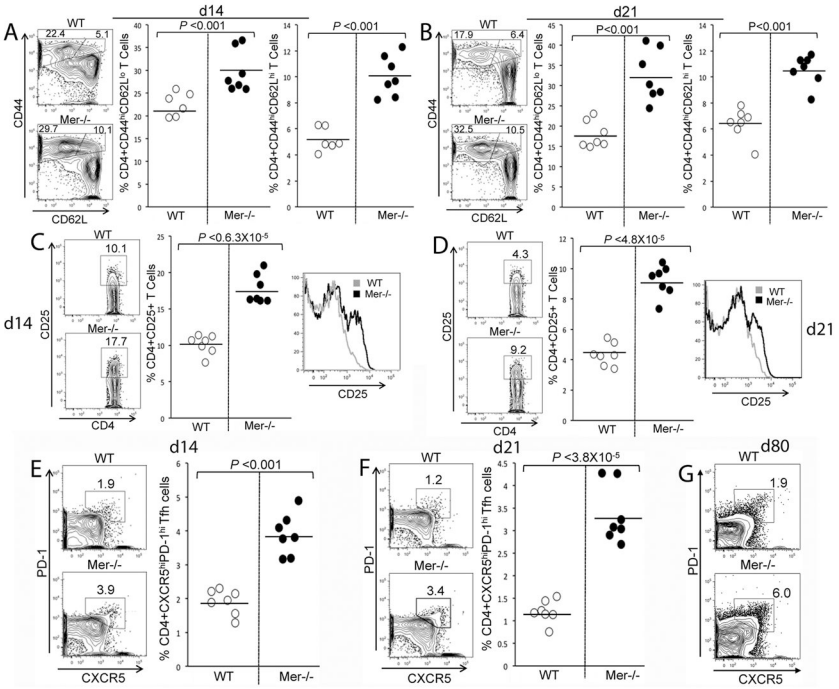

Figure 7. CD4$^+$ T cell responses are augmented in Mer−/− mice

Splenocytes obtained from WT and Mer−/− mice at day 14 (A and C) and 21 (B and D) post-immunization were stained with Abs against CD4, CD44, CD25 (IL-2Rα) and CD62L, and analyzed by flow cytometry. The percentage of CD4$^+$CD44^{hi}CD62L^{lo}(middle panels) and CD4$^+$CD44^{hi}CD62L^{hi} (right panels) T cells in WT (open circle) and Mer−/− (closed circle) mice is shown in (A) and (B). (C, D) Percentage of CD4$^+$CD25$^+$ T cells (defined by rectangular gates in left panels) in WT (open circle) and Mer−/− (closed circle) mice is shown in scatter plots (middle panels). The levels of CD25 on CD4 gated T cells from WT (gray line) and Mer−/− (black line) mice are shown in overlaid histograms (right panels). (E, F) Splenocytes obtained from WT and Mer−/− mice at day 14 (E) and 21 (F) post-immunization were stained with antibodies against CD4, PD-1 and CXCR5 and analyzed by flow cytometry. The percentage of CD4$^+$ CXCR5^{hi}PD-1^{hi} T_{FH} cells (defined as cells in polygonal gates, contour plots) in WT (open circle) and Mer−/− (closed circle) mice is shown in right panels (E, F). Horizontal bars represent the average values. Data were obtained from sex and age-matched seven mice of each genotype. (G) Similar analysis as in (E, F) was performed at day 80 on pooled samples of seven WT control (upper panel) and four Mer−/− (lower panel) mice.

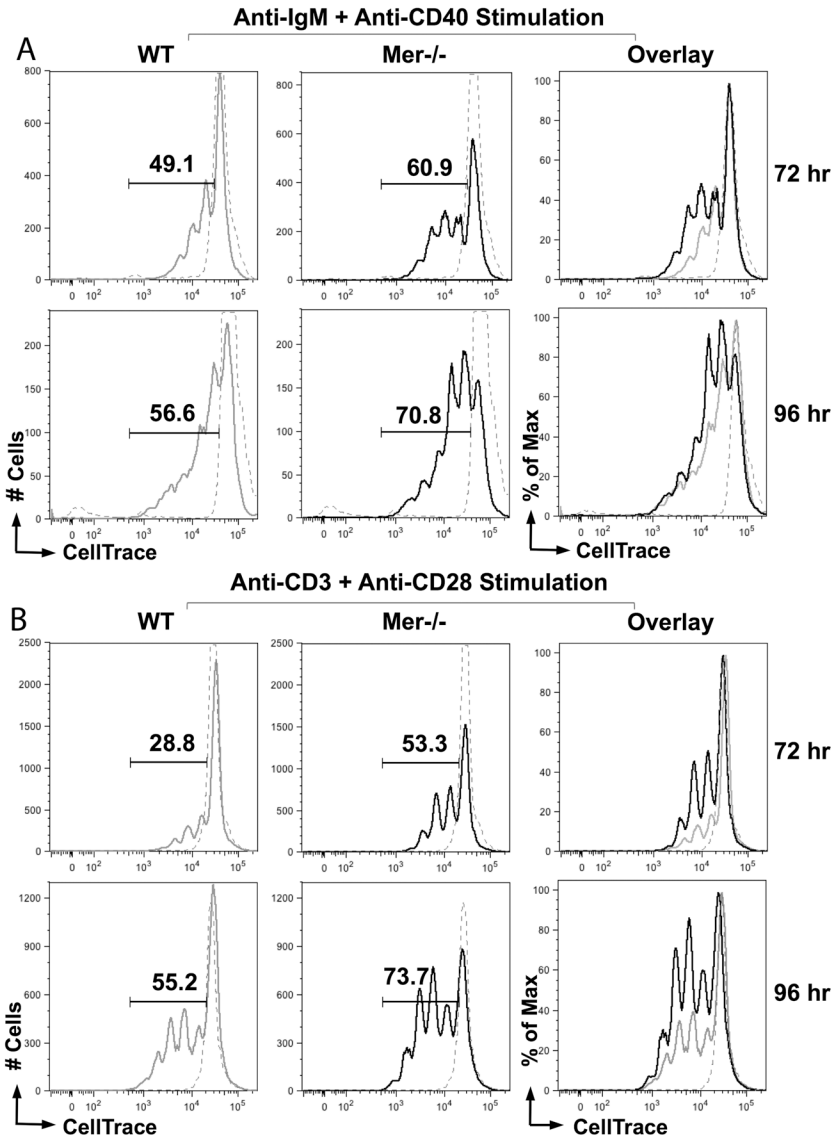

Figure 8. Mer deficiency drives faster proliferation in lymphocytes upon ex vivo stimulation

Representative flow cytometric histograms showing the quantification of proliferating cells from WT and Mer−/− mice by CellTrace violet dilution (x-axis) in B cells stimulated with anti-IgM and anti-CD40 antibodies (A), and T cells stimulated with anti-CD3 and anti-CD28 antibodies (B) at 72 hr (upper panels, A and B) and 96 hr (lower panels, A and B). Gate and numbers in each panel indicate the percentage of cells with decreased CellTrace Violet fluorescence intensity indicating proliferation. Solid grey line represents WT; solid black line, Mer−/−; dashed grey line, unstimulated cells. An overlay of these three histograms is shown in the right panel. These data are representative of two independent experiments each performed using cells pooled from at least 5 mice per group.

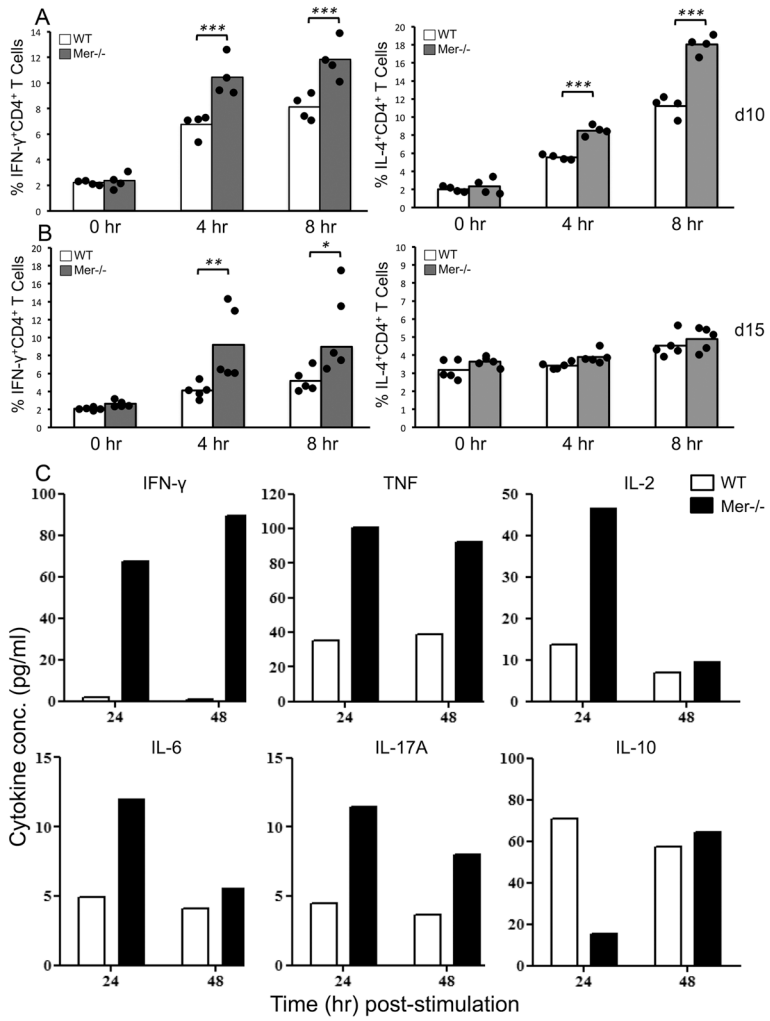

Figure 9. Increased IFN-γ production by CD4$^+$ helper T cells in NP-OVA immunized Mer−/− mice

(A, B) Intracellular cytokine flow cytometric analysis of CD4$^+$ helper T cells obtained from NP-OVA immunized 7–9 wk old WT and Mer−/− mice for IFN-γ left panels and IL-4 (right panels) at indicated days after immunization. Splenocytes were stimulated with PMA and Ionomycin for 0, 4, or 8hr *ex vivo* after isolation on days 10 and 15 post-immunization. Mean values are shown in bars (WT, open; Mer−/−, solid gray) and each circle overlayed on the bars represents an individual mouse. (C) Flow cytometric quantification of indicated cytokines in culture supernatants of purified T cells pooled from NP-OVA immunized 5 WT (open bars) and 5 Mer−/−(solid bars) mice, stimulated with PMA and Ionomycin for 24hr and 48hr. Concentration in pg/ml reflects the mean of at least two dilutions per sample. T cells were purified from Mer−/− and WT control mice 10 days post-immunization.

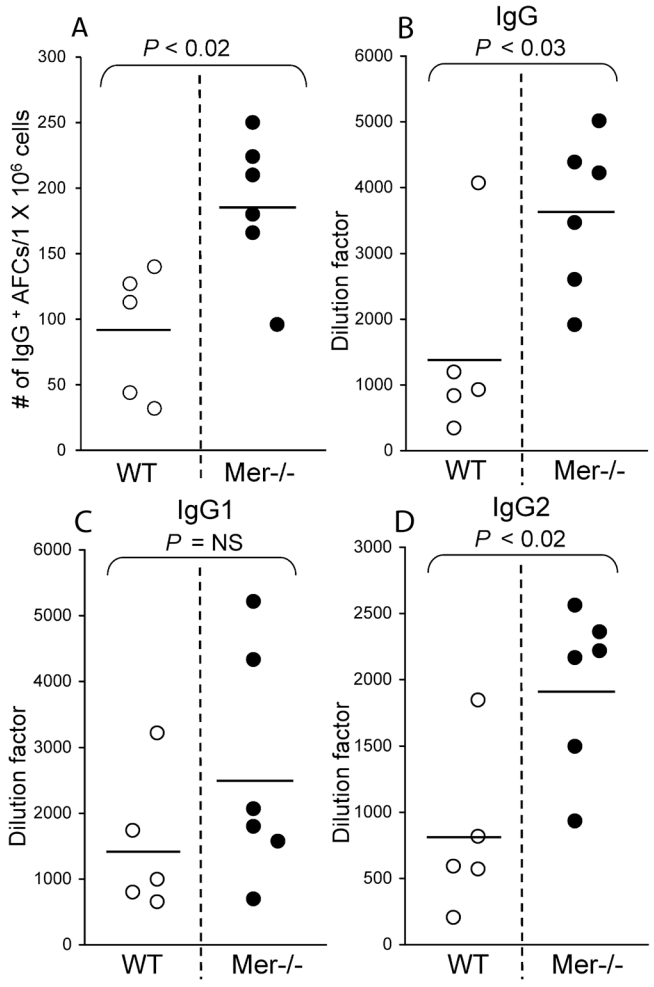

Figure 10. Augmented secondary AFC and IgG2 Ab responses in Mer−/− mice

(A) IgG-producing secondary AFCs in the spleen were measured by ELISpot assay four days after boosting WT (open circle) and Mer−/− (closed circle) mice with NP-OVA. Anti-NP IgG (B), IgG1 (C) and IgG2 (D) Ab titers were measured by ELISA in serum samples collected from mice described in (A). Each circle represents the number of AFCs per 1×10^6 splenocytes or Ab titers obtained from an individual mouse. Bars represent the mean values. Age- and sex-matched five to six mice of each genotype were used to generate these data.